Talanta xxx (xxxx) 122162

Contents lists available at ScienceDirect

Talanta

journal homepage: www.elsevier.com/locate/talanta

Exploring quantitative cellular bioimaging and assessment of CdSe/ZnS quantum dots cellular uptake in single cells, using ns-LA-ICP-SFMS

J. Pisonero [a, *], H. Traub [b], B. Cappella [b], C. Álvarez-Llamas [c], A. Méndez [a], S. Richter [b], J. Ruiz Encinar [d], J.M. Costa-Fernandez [d], N. Bordel [a]

[a] Department of Physics, University of Oviedo, C/ Federico García Lorca, Nº18, 33007, Oviedo, Spain
[b] Bundesanstalt für Materialforschung und -prüfung, (BAM), Unter Den Eichen 87, 12205, Berlin, Germany
[c] Department of Analytical Chemistry, University of Malaga, 29071, Málaga, Spain
[d] Department of Physical and Analytical Chemistry, University of Oviedo, Avda. Julian Claveria, 8, 33006, Oviedo, Spain

ARTICLE INFO

Keywords:
LA-ICP-SFMS
Fast single pulse response
Quantitative bioimaging
Cellular uptake
HT22
HeLa
Single cell
pL-droplets
CdSe/ZnS quantum Dots
AFM

ABSTRACT

Quantitative bioimaging of Quantum Dots (QDs) uptake in single cells by laser ablation inductively coupled plasma mass spectrometry (LA-ICP-MS) is a challenging task due to the high sensitivity and high spatial resolution required, and to the lack of matrix-matched reference materials. In this work, high spatially resolved quantitative bioimaging of CdSe/ZnS QDs uptake in single HT22 mouse hippocampal neuronal cells and in single HeLa human cervical carcinoma cells is novelty investigated combining: (a) the use of a ns-LA-ICP-Sector Field (SF)MS unit with mono-elemental fast and sensitive single pulse response for $^{114}Cd^{+}$; and (b) the spatially resolved analysis of dried pL-droplets from a solution with a known concentration of these QDs to obtain a response factor that allows quantification of elemental bioimages. Single cells and dried pL-droplets are morphologically characterized by Atomic Force Microscopy (AFM) to determine their volume and thickness distribution. Moreover, operating conditions (e.g. spot size, energy per laser pulse, etc.) are optimized to completely ablate the cells and pL droplets at high spatial resolution. Constant operating conditions for the analysis of the single cells and calibrating samples is employed to reduce potential fractionation effects related to mass load effects in the ICP. A number concentration of CdSe/ZnS QDs between 3.5 10^4 and 48 10^4 is estimated to be uptaken by several selected single HT22 and HeLa cells, after being incubated in the presence of a QDs suspension added to a standard cell culture medium. Mono-elemental bioimaging at subcellular resolution seems to show a higher number concentration of the CdSe/ZnS QDs in the cytosol around the cell nucleus.

1. Introduction

Associated with the growing use of engineered nanomaterials in consumer products, electronics, and pharmaceuticals the nano-bio interaction has become more and more into focus [1–3]. As a special kind of nanomaterials, inorganic semiconductor nanoparticles, known as quantum dots (QDs), are today widely applied in scientific research, bioanalytical applications and industrial applications due to their unique optical and electrical properties. QDs hold great promise in biotechnology and biomedicine, for example as artificial tags for biomolecule labelling, in vivo imaging and cell tracking experiments.[4,5] However, several studies have indicated a potential risk of the use of the more conventional Cd-based QDs to the environment and living organisms under certain circumstances [6]. In this context, *in vitro* studies are frequently used to study the cellular uptake and processing of nanomaterials in biological systems. Therefore, numerous analytical methods have been developed or improved to allow the analysis of individual cells and cell compartments [7,8].

Quantification of nanoparticles (NPs) in cells has been generally investigated by digesting a cell suspension or pellet [9]. However, by averaging over such a huge ensemble of cells all individual variations are getting lost. Single cell analysis by Inductively Coupled Plasma Mass Spectrometry (SC-ICP–MS) might be achieved operating in a time-resolved mode so that the frequency of signals is directly related to the number concentration of cells and the intensity of signals is related to intracellular amount of elements [10]. Nevertheless, no information about the NP distribution within a single cell is available. Moreover, in spite of the small size of QDs nanoparticles (typically of only few

* Corresponding author.
E-mail address: pisonerojorge@uniovi.es (J. Pisonero).

https://doi.org/10.1016/j.talanta.2021.122162
Received 27 November 2020; Received in revised form 12 January 2021; Accepted 25 January 2021
0039-9140/

nanometer size) and the heterogeneous composition (made of a core comprising several elements, e.g. ZnS/CdSe) sometimes sensitivity of sp-ICP-MS is not good enough to allow a reliable NP quantitation.

Other methods, such as cell staining with metal and semiconductive nanoparticles are promising for imaging applications due to its high spatial resolution and high sensitivity. For instance, the use of microscopic cell staining with photoluminescence semiconductive quantum dots or carbon-dots allows the employment of photoluminescence techniques for qualitative and quantitative imaging applications, even during real time monitoring [11]. Complementarily, Laser Ablation (LA)-ICP-MS is a very sensitive technique that allows the micro-spatially resolved determination of trace elements, and it is not limited to the detection of photoluminescence species [12–15].

Recent advances in LA-ICP-MS based on the development of ablation chambers with very short aerosol wash-out times make this technique more and more attractive for multiple applications, including the localization and quantification of receptor-specific tracers [16], or bioimaging using metal-tagged antibodies [17,18]. However, one of the main drawbacks of the fast wash-out chambers in LA-ICP-MS for multielemental analysis is the requirement of a high mass spectra acquisition rate spectrometer. ICP-Time-of-Flight MS might be the most adequate candidate as it is able to provide complete mass spectra at acquisition rates ≥30 kHz [19]. Nevertheless, sequential mass spectrometers, such as ICP-Sector Field (SF)MS provides better sensitivity and might be optimized for fast, sensitive and high spatially resolved single elemental analysis [20]. It should be remarked that a reduction of the laser spot size (e.g. spots of a few micrometers are required for cell imaging) is inherently related to a loss in sensitivity due to the fact that the amount of material ablated and thereby the number of atoms entering the ICP-MS is reduced.

Quantitative bioimaging analysis using LA-ICP-MS requires high sensitivity, high spatial resolution and an appropriate quantification method. In this sense, multiple approaches have been investigated as calibrations methods. Among the most popular methods, it should be highlighted the use of: thin layers of spiked agarose gels [21], spiked gelatin gels (air-dried or oven-dried) [22], standards spotted onto nitrocellulose membrane [23], or dried pL-droplets from calibrating samples [24,25]. Ideally, LA-ICP-MS operating conditions (e.g. spot size, energy per laser pulse, etc.) should be constant during the analysis of the cells and calibrating samples, in order to reduce/avoid fractionation effects due to mass load effects at the plasma site [26]. However, not all these calibrating samples are properly ablated using the low laser fluence energy required for the high spatial resolved analysis of the cells. Dried pL-droplets, from solutions containing Rhodamine B as a carbon source to match the matrix of single cells, are typically fully ablated using large laser-induced spot sizes (>100 μm), but they are also soft enough to be ablated line by line using low laser fluence conditions and small laser-induced spot sizes (<4 μm).

Uptake and biodistribution of Cd-based QDs within cells is increasingly studied due to fact that their constituents (Cd and Se) are known to cause acute and chronic toxicities in vertebrates [27,28]. Therefore, in this work, high spatially resolved quantitative bioimaging of Cd-based QDs uptake in single HT22 mouse hippocampal neuronal cells and in single HeLa human cervical carcinoma cells is investigated making use of a ns-LA-ICP-SFMS unit with fast single pulse response. Moreover, dried pL-droplets from solutions with a known concentration of Cd-based QDs are evaluated to obtain a response factor that allows quantification of elemental bioimages. LA-ICP-MS operating conditions are optimized to completely ablate the cells and pL droplets at high spatial resolution. Complementary morphological information from cells and dried pL-droplets is obtained by Atomic Force Microscopy (AFM).

2. Experimental

2.1. Ns-LA-ICP-SFMS

A NWRimage laser ablation system from Elemental Scientific Inc. (ESI, Bozeman, MT,USA) was used in combination with an ultra-fast wash-out ablation chamber (Bloodhound) and a Dual Concentric Injector (DCI). Moreover, the laser-induced aerosol is transported from the sniffer (inner micro sampling chamber) to the ICP-SFMS through a flexible silicon tube (<1 m length and 1.7 mm i. d). The detection was carried out by an Element XR ICP-SFMS (Thermo Fisher Scientific, Bremen, Germany). More details about this LA-ICP-SFMS experimental set-up that provides fast single pulse response could be found elsewhere [20] Operation conditions in the ICP-MS (e.g. ion optics, gas flows). Were daily optimized. The ion optic was adjusted to obtain the maximum sensitivity monitoring $^{137}Ba^+$ and $^{232}Th^+$ signals produced by the ablation of the standard reference material NIST 612 in scanning mode at 50 Hz, 60 μm spot size, 10 μm/s and maximum fluence (20 J/cm^2). Additionally, the sample gas flow was also adjusted to keep the ratios $^{238}U^+/^{232}Th^+$ and $^{248}OTh^+/^{232}Th^+$ below 120% and 0.7 %, respectively. A low roughness surface sample consisting of Indium Tin Oxide (ITO) layer, deposited on a glass substrate, was employed to optimize the distance between the sniffer and the surface of the sample, in terms of ion signal ($^{120}Sn^+$) and wash-out time after each ablation event as described in [20].

High purity Ar (99.999% minimum purity) from Linde (Germany) was employed as plasma and sample gas. Ar was coaxially mixed with the He (99.999%, Linde, Germany) carrier gas inside the DCI before entering the ICP. The calibration of the digital and analogous detectors was carried out daily to warrant a linear response in the detection.

Element XR provides excellent sensitivity but it is a relatively slow sequential mass analyzer; therefore, the acquisition conditions of the ICP-SFMS were optimized for faster mass spectra acquisition rate, collecting ion signals (every 2 ms) in low resolution mode within the flat top peak of the corresponding isotope (note that fast acquisition conditions might be affected when operating the SFMS in middle or high resolution). Table 1 lists the optimized operating conditions of the ns-LA-ICP-SFMS system.

2.2. AFM

Atomic force microscopy (AFM) measurements were performed in contact mode with a Cypher microscope (Asylum Research, Santa Barbara, CA, USA). For the AFM measurement of the dried droplet the instrument was equipped with a NSC15 cantilever (silicon cantilever, MicroMasch, Tallinn, Estonia) and contact mode was used, while for the measurement of the cells a very soft cantilever CSC12 (silicon cantilever) was employed in contact mode.

2.3. Chemicals, cell culture and treatment

All the chemical reagents used in the experiments were of analytical grade and used as received without further purification. Deionized ultrapure water (18.2 MΩ cm) was obtained with a PURELAB flex system (ELGA LabWater, UK).

CdSe/ZnS quantum dots surface functionalized with carboxyl groups for stabilization in aqueous media (QDs, Qdot® 605 ITK™ carboxyl quantum dots) were purchased from Invitrogen-Molecular Probes (Thermo Fisher Scientific; Eugene, OR, USA). Such QDs have a nanocrystaline core of a semiconductor material (CdSe), which are shelled with an additional semiconductor layer (ZnS) to improve their optical properties [29]. These QDs have an inorganic core diameter of 4 nm and have been extensively used as highly valuable fluorescent probes for the imaging of biological samples [30]. A stock solution was

Table 1
Operating conditions of the ns-LA-ICP-SFMS.

Laser ablation unit	
Laser wavelength/nm	266 (Nd:YAG (4th harmonic))
Laser frequency/Hz	100
Nominal spot size/μm	2
Measured spot size at the surface/μm	<4
Scanning speed/μm s^{-1}	50
Fluence/J cm^{-2}	0.1
He carrier gas flow rate/L min^{-1}	1.5
Wash-out time/ms	~15
ICP-SFMS	
RF power/W	1350
Guard electrode	Platinum, active
Ar cooling gas flow rate/L min^{-1}	16
Ar auxiliary gas flow rate/L min^{-1}	1.0
Ar sample gas flow rate/L min^{-1}	0.6–0.8
Sample and skimmer cone	Ni
Mass resolution	Low (R = 300)
Scan optimization	Speed
Isotopes monitored	^{120}Sn, ^{114}Cd (only one isotope per analysis)
Magnet settling time/s	0.001
Runs x pass	Depends on the size of the region of interest: from 14 × 1 to 24 × 1.
Detection mode	Triple (isotopes measured with SEM)
Sample time/s	0.002
Samples per peak	1000
Segment duration/s	0.4
Mass window/%	20
Search window/%	0
Integration window/%	20
Scan type	E-scan

prepared, dispersing these carboxyl QDs in 50 mM borate (pH 9.0) at a molar nanoparticle concentration number of 100 nM.

HT22 mouse hippocampal neuronal cells were obtained from The Salk Institute, San Diego, CA, USA; while human cervical carcinoma cells (HeLa cells; Cat Number #CCL-2™) were obtained from the 'American Type Culture Collection' (ATCC; Manassas, VA, USA). Cells were cultured in Dulbecco's Modified Eagle Medium (DMEM) supplemented with 10% fetal bovine serum (FBS), 2 mM L-glutamine, 10 mM HEPES and an antibiotic-antimycotic cocktail containing 100 U/mL penicillin, 10 μg/mL streptomycin and 0.25 μg/mL amphotericin B. All cell culture reagents were purchased from Gibco®-Invitrogen (Thermo Fisher Scientific; Waltham, MA, USA), unless otherwise indicated. Cells were maintained in T75 flask under a 5% CO2 atmosphere at 37 °C and split twice a week by trypsinization before confluency.

For LA-ICP-SFMS experiments, cells were seeded at a density of 10 000 cells/mL and grown on sterile Nunc™ Thermanox™ coverslips, from Thermo Fisher Scientific, in a 12-well plate. Then, cells were incubated with a QDs suspension at a nanoparticle concentration of 6 nM in standard cell culture medium. After an exposure time of 24 h, cells were rinsed with phosphate buffered saline (PBS) and immediately fixed with 4% formaldehyde in PBS. After fixation, cells were dehydrated in a graded series of ethanol (30% 50%, 70%, 90% and two times 100%; at least 1 min residence time in every solution) and, finally, dried for LA-ICP-SFMS analysis.

2.4. pL-droplets generator

For the quantification of the QDs in the cells the CdSe/ZnS nanoparticles suspension was spotted in pL droplets on microscope slides (Superfrost Plus, Thermo Scientific). The composition of the pL droplets consists of the original QD stock solution diluted to a final nanoparticle concentration number of 10 nM using a 0.5 wt% Rhodamine B (Rhodamine B powder, ≥ 95%, Sigma Life Science, Munich, Germany) solution in deionized ultrapure water (MilliQ system, Merck Millipore, Darmstadt, Germany). Moreover, the diluted QD stock solution was homogenized before sampling by mixing for 1 min using an Analog Vortex Mixer (VWR, Dresden, Germany). According to Wang et al. [31] Rhodamine B was added to the QD solutions as a carbon source to match the matrix of single cells. Besides, Rhodamine B allows the visualization of the pL droplets after spotting on a glass slide due to its magenta color. For the spotting process a micro array spotter (sciFLEXARRAYER S3, Scienion AG, Berlin, Germany) equipped with a piezo dispense capillary (PDC 70, coating type 3) was employed. An average droplet volume per spot of 293 pL ± 20 pL was gravimetrically determined based on 10 000 droplets according to Ref. [22].

3. Results and discussion

3.1. Elemental distribution of Cd-based QDs in single cells using ns-LA-ICP-SFMS

The combination of high laser repetition rate, high scanning speed and small laser spots results in fast and highly spatially resolved analysis. Additionally, the main advantages from the use of fast wash-out ablation chambers (< 30 ms) include: reduced aerosol dispersion, which minimizes the intermixing of the ablated material generated from consecutive laser shots when operating the laser at high repetition rates (~100 Hz); and high ion signal to background ratios due to fast single pulse response.

The elemental distributions of Cd-based QDs in HT22 and HeLa single cells, after growing the cells in a culture media enriched with the QDs, were measured using ns-LA-ICP-SFMS at the operating conditions listed in Table 1. Ablation was carried out in scanning mode and using parallel and adjacent ablation lines (separated by 2 μm). Cross-profiles of the laser-induced ablated lines in the samples were measured using AFM. Fig. S1 (supplementary figure) shows the formation of a laser-induced Gaussian shape channel with a depth of about 1.4 μm and a surface diameter of 4 μm. Moreover, Fig. S2 (supplementary figure) shows the morphology and dimensions of a fixed and dried HT22 cell measured by AFM; showing a maximum thickness of about 1.2 μm. Xiaoling Yun et al. [32] measured similar maximum thickness for the HeLa cells using another AFM set-up. Therefore, at the selected operating conditions, laser-induced scanning lines are considered to completely ablate a small part of the cells with each single laser shot.

Qualitative distribution of $^{114}Cd^+$ ion signals from the core of the QDs was measured with sub-cellular resolution. Before each ablation line, background $^{114}Cd^+$ ion signal (with no ablation) was measured to be subtracted afterwards. Fig. S3 (top, left and right) (supplementary figure) shows the bright field image of two single fixed HT22 cells, and the ns-LA-ICP-SFMS image of the $^{114}Cd^+$ intensity distribution superimposed on the bright field image, respectively. It is observed that relevant LA-ICP-SFMS ion signals were detected inside the cells. Variation of $^{114}Cd^+$ along an axis crossing both cells (see red line in Fig. S3 (top, right)) is plotted in Fig. S3 (bottom) to illustrate the values of ion signal (cps) within the cells and in the region between both of them. An analogous distribution of $^{114}Cd^+$ ion signals was measured in the HeLa cells (see Fig. S4).

3.2. Quantitative uptake of Cd-based quantum dots in single cells, using ns-LA-ICP-SFMS

Quantitative uptake of Cd-based quantum dots in single cells require the use of a proper calibration strategy to obtain a response factor (e.g. relationship between the measure ion signal and the number of QDs). Ideally, this methodology requires the use of a reference sample that can be considered as a matrix-match; constant operating condi-

tions for the sample and for the reference sample to obtain similar mass load effects at the ICP; quantitative ablation of the standard analyte to establish the direct link between mass loaded and signal obtained; and quantitative ablation of the sample under the same conditions to allow the use of the response factor obtained with the refence sample.

In this context, the use of pL-droplets from a known QDs solution is considered as a calibrating sample that satisfies these conditions. Initially, dried 293 ± 20 pL-droplets from a 10 nM Cd-based QDs solution, containing Rhodamine B as a carbon source to match the matrix of single cells, were morphologically characterized using AFM. Fig. 1 shows: (a) stitched AFM images of a horizontal section of the pL-droplet, and (b) the profile along the x axis at y = 15.17 μm. These dried pL-droplet have a circular shape with a diameter of about 150 μm. Moreover, it is observed that the pL-droplets concentrate most of their volume at the edges. This heterogenous distribution observed in the dry pL-droplet is associated to "coffee-stain" and "Marangoni" effects. Therefore, the maximum thickness of the dried droplet is measured to be < 150 nm and at the edges.

Droplets were completely ablated by parallel and adjacent line scans, using the same operating conditions as for the analysis of the HT22 and HeLa cells. Nevertheless, it has to be noted that these operating conditions were below the ablation threshold value for other calibration samples, such as doped agarose gels (1000 pg Cd/mm^2) prepared according to [21]. Fig. 2 shows a bright-field image of a partially ablated pL-droplet. Additionally, Fig. 3 shows the qualitative distribution of $^{114}Cd^+$ ns-LA-ICP-SFMS ion signals in the pL-droplets from 10 nM Cd-based QDs solution, measured with high spatial resolution (<4 μm). It is observed that $^{114}Cd^+$ ion signals are enhanced at the edges of the droplet, where most of the volume of the dried droplet is concentrated. Total ion signal per droplet was measured integrating $^{114}Cd^+$ion signals within the droplet area. Moreover, background $^{114}Cd^+$ ion signals were obtained from the analysis, at the same operating conditions, of an outer region with the same area as the droplets. Total net ion signal was then calculated after subtraction of background signal. Afterwards, the response factor was calculated as the ratio of the net integrated ion signal from the 293 ± 20 pL-droplets (10 nM QDs solution), and the number of CdSe/ZnS QDs contained in that droplets. Table 2 lists the integrated $^{114}Cd^+$ signal (cps) in the pL-droplets from the 10 nM QDs solution, the net $^{114}Cd^+$ signal (cps), the number of QDs in the pL droplet (#), and the calculated response factor (cps/QDs). It is noticed that the low concentration of QDs in the pL-droplet and their accumulation at the edges of the droplet resulted in weak signal compared to the background level. The response factor was estimated to be 418 ± 32 cps of $^{114}Cd^+$ net ion signal per CdSe/ZnS QD.

3.3. Quantitative uptake of Cd-based QDs in HT22 cells and HeLa cells

Distribution of $^{114}Cd^+$ ion signals at subcellular level can be converted into quantitative distribution of CdSe/ZnS quantum dots in single cells, multiplying the net intensity (after background subtraction) by the inverse of the calculated response factor. Fig. 4 shows the distribution of number of CdSe/ZnS QDs in: (a) two HT22 mouse hippocampal neuronal cells; (b) nine HeLa human cervical carcinoma cells. A logarithmic color-based scale is employed to highlight the number concentration of CdSe/ZnS QDs on the different parts of the cells, which varies between 0 and 330. It is observed that for both type of cells the accumulation of CdSe/ZnS QDs typically takes place around the cell nucleus. This finding is in accordance with Jiang et al. [33], who detected an active transport of QD containing endosomes toward the perinuclear region. The Cd signals in the nucleus area can be attributed to QDs in the cytoplasm below and above the cell nucleus. Moreover, an anomaly was observed at the left-hand side of Fig. 4(b), where three HeLa cells were found to contain significantly lower amounts of Cd-based QDs. The reasons for this finding might include different phase in their cell cycle as the cells were not synchronized.

Furthermore, assessment of cellular uptake of CdSe/ZnS quantum dots in single cells can be obtained integrating the number of QDs on each cell in Fig. 4. Tables 3 and 4 list the net integrated $^{114}Cd^+$ ion signal and the total number of CdSe/ZnS QDs per cell, measured for the HT22 and HeLa cells, respectively. It is noticed that the total number of QDs per cell in both types of cells, cultured at the same conditions, was determined to be between 3.5 10^4 and 48 10^4, showing cell to cell variability.

Obviously, the number of QDs internalized per cell will depend on the type of cell and concentration of QDs used. Previous studies carried

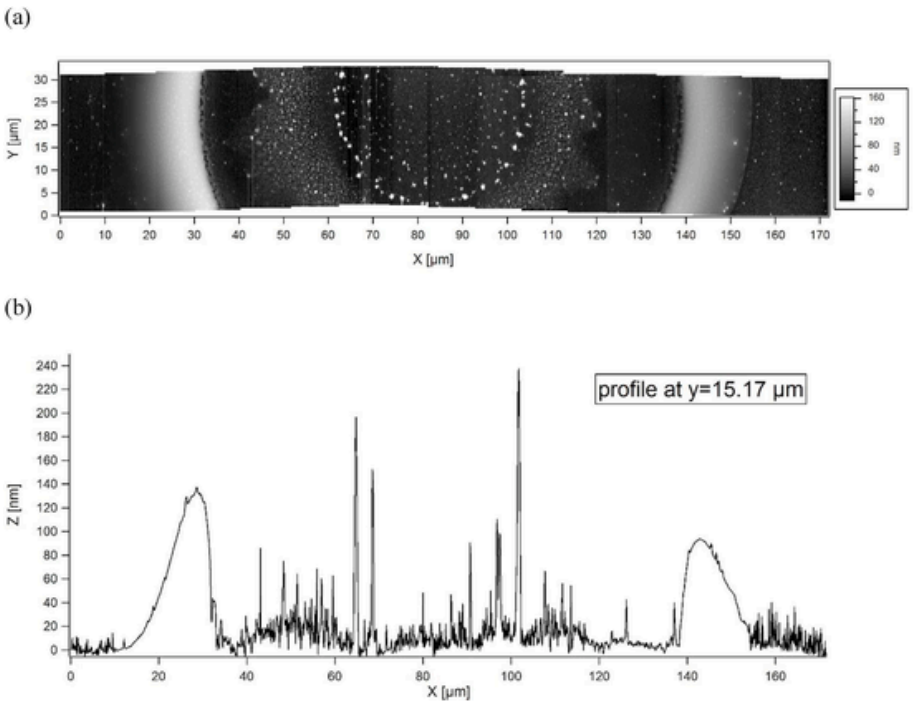

Fig. 1. (a) Stitched AFM topographies of a horizontal section of the pL-droplet. (b) Line profile along the x axis at y = 15.17 μm in AFM topography.

Fig. 2. Bright-field image of a partially ablated pL-droplet.

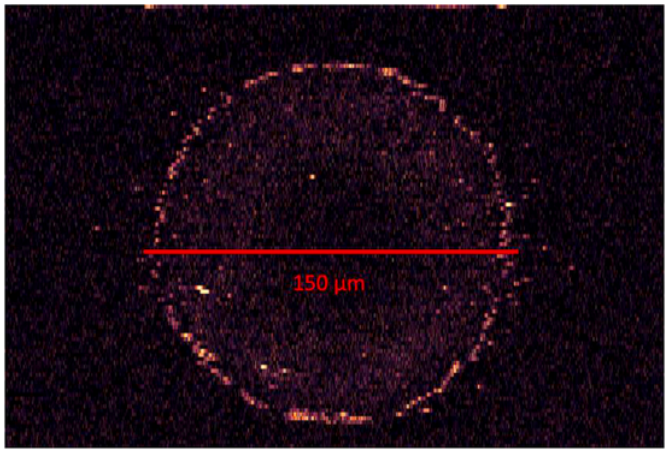

Fig. 3. LA-ICP-SFMS image of the smoothed $^{114}Cd^+$ intensity distribution (distribution of Cd-based QDs) inside a pL-droplet from a 10 nM Cd-based QDs solution.

Table 2
Measured $^{114}Cd^+$ integrated intensities of 293 ± 20 pL-droplets (from 10 nM QDs solution) (cps), net $^{114}Cd^+$ integrated signal (cps), number of Cd-QDs in the pL-droplet (#), calculated response factor (cps/CdQDs).

	$^{114}Cd^+$ Integrated intensity (cps)	$^{114}Cd^+$ Net Signal (cps)	Number of Cd-QDs in doped pL droplet	Response Factor (cps/# CdQDs)
pL-droplet #1 (from 10 nM QDs solution)	$2.20\ 10^9$	$7.62\ 10^8$	$1.76 \pm 0.12\ 10^6$	418 ± 32
pL-droplet #2 (from 10 nM QDs solution)	$2.16\ 10^9$	$7.14\ 10^8$	$1.76 \pm 0.12\ 10^6$	

out by Z. Ling-Na et al. [34], using single cell (SC)-ICP-MS were used to determine intracellular CdSe/ZnS QDs in single cells (Raw 264.7 cells, a mouse leukemic monocyte macrophage cell line) after exposure. They measured an increasing number of QDs per cell at higher incubation times, observing about $6\ 10^4$ QDs/cell after 12 h of incubation. This value could be extrapolated to $>10\ 10^4$ QDs after 24 h of incubation, which was the incubation time employed in this study. In any case, caution must be exercised because many authors highlight the strong dependence of this incorporation on the cell and QDs type (e.g. uptake of QDs by cells is considered to be mainly determined by the surface-modification of the QD surface and by the nanoparticle shape and size) [35,9].

4. Conclusions

High spatially resolved quantitative bioimaging achieved by ns-LA-ICP-SFMS with fast mono-elemental single pulse response was used to assess the CdSe/ZnS QDs uptake and distribution in single HT22 mouse hippocampal neuronal cells and in single HeLa human cervical carcinoma cells. Operating conditions were optimized to completely ablate the cells at high spatial resolution (< 4 µm) and to achieve a high-sensitive distribution of $^{114}Cd^+$ ion signals within these cells. Multielemental analysis at high speed and at high spatial resolution, using for instance LA-ICP-TOFMS, could be employed to confirm that ion signals come from the QDs. Nevertheless, the multi-element information obtained using TOF will come with a significant decrease in sensitivity in comparison to SF, even compromising the detection of the QDs.

Atomic Force Microscopy (AFM) was used to determine the ablation rate and morphology (including sample thickness) of the cells, and thus to validate the efficiency of the ablation process. As calibrating samples pL-droplets from a solution containing QDs and Rhodamine B as a carbon source to match the matrix of single cells, were employed. AFM was also used to determine the morphology of the pL-droplets. In the investigated method, the pL-droplet were ablated at the same high spatial resolution conditions as the cells. In this initial exploratory study a reduced number of pL-droplets, from a solution with constant 10 nM concentration of CdSe/ZnS QDs, were analysed to estimate a response factor of the analytical method, which was calculated as the ratio of the net integrated $^{114}Cd^+$ ion signal from the pL-droplets and the number of CdSe/ZnS QDs contained in that droplets, resulting in a value of 418 ± 32 cps/QD. Further studies will be performed using multiple pL-droplets from solutions with different molar concentration of QDs in order to validate these results and to explore in more detail the analytical capabilities of this method (e.g. limits of detection, linear dynamic range, etc.).

Using the estimated response factor, the qualitative distribution of $^{114}Cd^+$ ion signals at subcellular level were converted into quantitative distribution of CdSe/ZnS quantum dots in single cells. Nevertheless, it should be remarked that there is still a limited spatial resolution (due to the use of laser spot sizes < 4 µm and some overlapping) to achieve a further detail subcellular distribution of quantum dots uptakes.

For both type of cells, the internalized CdSe/ZnS QDs were distributed in the cytosol around the cell nucleus. Furthermore, assessment of cellular uptake of CdSe/ZnS quantum dots in single cells was obtained directly integrating the number of QDs on each cell. The total number of QDs per cell in both types of cells (HT22 and HeLa cells), cultured at the same conditions, was determined to be between $3.5\ 10^4$ and $48\ 10^4$, showing cell to cell variability. It should be remarked that these biological uncertainties (e.g. variation in uptake of QDs), already observed for this reduced number of cells, were significantly higher than the uncertainties given by the analytical method. In this sense, studies with a larger number of cells will be performed to obtained comprehensive assessment of CdSe/ZnS quantum dots cellular uptake in single cells.

Credit author statment

J. Pisonero: Conceptualization, Methodology, Investigations, Writing, Supervision. H. Traub: Methodology, Investigation, Writing. B. Cappella: Investigation. C. Álvarez-Llamas: Data curation. A. Méndez: Data curation. S. Richter: Resources. J. Ruiz Encinar: Writing-Reviewing. J.M. Costa-Fernandez: Writing-Reviewing. N. Bordel: Writing-Reviewing.

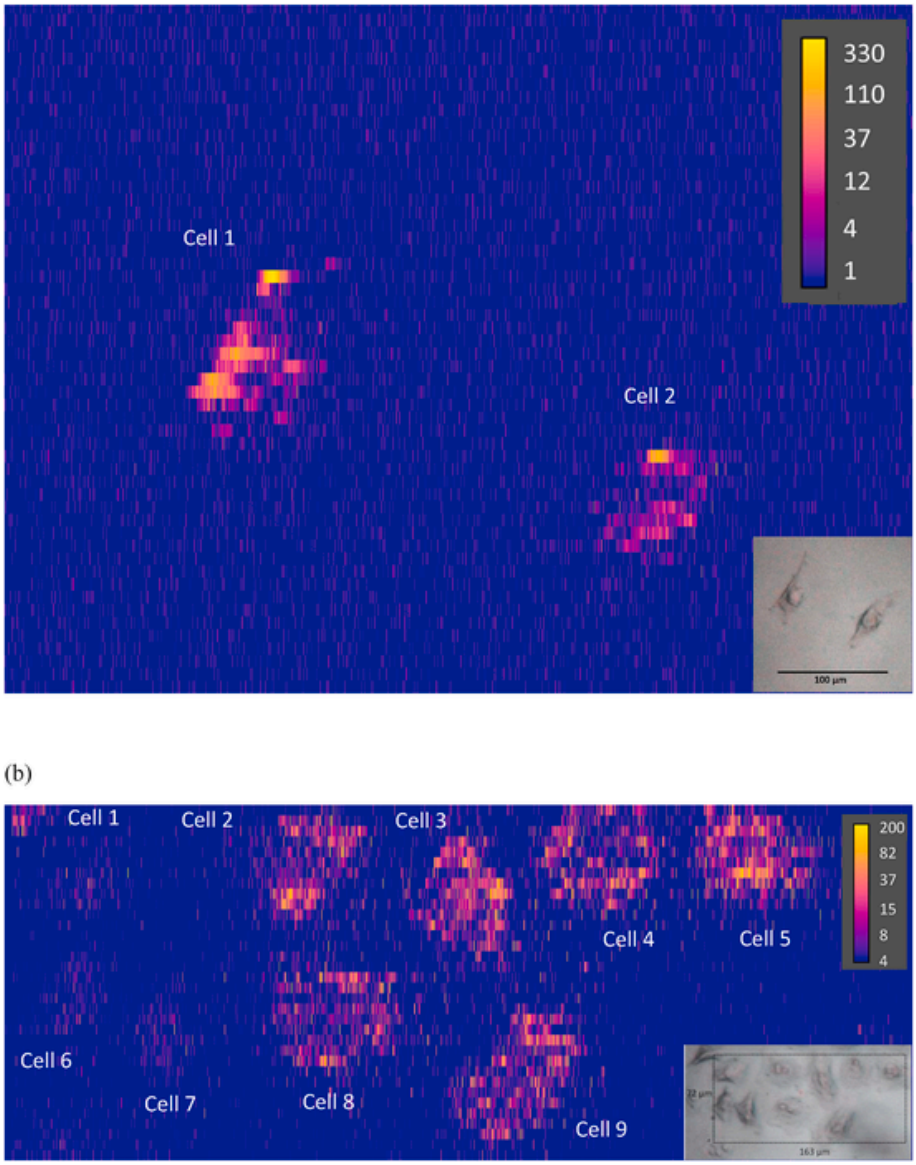

Fig. 4. Distribution of number concentration of CdSe/ZnS quantum dots in: (a) two HT22 mouse hippocampal neuronal cells; (b) nine HeLa human cervical carcinoma cells. Inlet figures show the bright-field images of the fixed cells before the ablation process.

Table 3
Net integrated $^{114}Cd^+$ intensities and total number of CdSe/ZnS QDs determined per cell at each measured HT22 cell.

HT22 Cell	Net Integrated $^{114}Cd^+$ intensity (cps)	Total number of CdSe/ZnS QDs per cell
1	$2.03\ 10^8$	$48 \pm 3\ 10^4$
2	$7.11\ 10^7$	$18 \pm 1\ 10^4$

Table 4
Net integrated $^{114}Cd^+$ intensities and total number of CdSe/ZnS QDs determined per cell at each measured HeLa cell.

HeLa Cell	Net Integrated $^{114}Cd^+$ intensity (cps)	Total number of CdSe/ZnS QDs per cell
1	$1.95\ 10^7$	$4.7 \pm 0.3\ 10^4$
2	$1.21\ 10^8$	$29 \pm 2\ 10^4$
3	$1.30\ 10^8$	$31 \pm 2\ 10^4$
4	$1.42\ 10^8$	$34 \pm 2\ 10^4$
5	$1.67\ 10^8$	$40 \pm 3\ 10^4$
6	$1.47\ 10^7$	$3.5 \pm 0.3\ 10^4$
7	$1.93\ 10^7$	$4.6 \pm 0.3\ 10^4$
8	$9.88\ 10^7$	$24 \pm 2\ 10^4$
9	$1.21\ 10^8$	$29 \pm 2\ 10^4$

Declaration of competing interest

The authors declare that they have no known competing financial interests or personal relationships that could have appeared to influence the work reported in this paper.

Acknowledgements

The authors would like to acknowledge the financial support from the Government of the Principality of Asturias through the projects IDI/2018/000186 and IDI/2018/000166 and from the Ministerio de Economia (Spain), through the national projects, MINECO-17-CTQ2016-77887-C2-1-R and MCI-20-PID2019-109698 GB-I00. Jorge Pisonero acknowledges support as Guest Scientist at the Bundesanstalt für Materialforschung und -prüfung (BAM). Furthermore, the authors would like to thank Jessica Saatz for providing the agarose gels, and Konrad Löhr for support with the microarray spotter.

Appendix A. Supplementary data

Supplementary data to this article can be found online at https://doi.org/10.1016/j.talanta.2021.122162.

References

[1] S. Behzadi, V. Serpooshan, W. Tao, M.A. Hamaly, M.Y. Alkawareek, E.C. Dreaden, D. Brown, A.M. Alkilany, O.C. Farokhzad, M. Mahmoudi, Cellular uptake of nanoparticles: journey inside the cell, Chem. Soc. Rev. 46 (2017) 4218–4244.

[2] Z. Gajdosechova, Z. Mester, Recent trends in analysis of nanoparticles in biological matrices, Anal. Bioanal. Chem. 411 (2019) 4277–4292.

[3] U.M. Graham, A.K. Dozier, G. Oberdorster, R.A. Yokel, R. Molina, J.D. Brain, J.M. Pinto, J. Weuve, D.A. Bennett, Tissue specific fate of nanomaterials by advanced analytical imaging techniques - a review, Chem. Res. Toxicol. 33 (2020) 1145–1162.

[4] A. Taylor, K.M. Wilson, P. Murray, D.G. Fernig, R. Lévy, Long-term tracking of cells using inorganic nanoparticles as contrast agents: are we there yet?, Chem. Soc. Rev. 41 (2012) 2707–2717.

[5] A.R. Montoro Bustos, M.T. Fernández-Argüelles, J. Ruiz Encinar, J.M. Costa Fernández, A. Sanz-Medel, Elemental mass spectrometry: a powerful tool for an accurate characterisation at elemental level of quantum dots, Chem. Commun. 47 (2009) 3107–3109.

[6] R. Hardman, A toxicologic review of quantum dots: toxicity depends on physicochemical and environmental factors, Environ. Health Perspect. 114 (2) (2006) 165–172.

[7] K. Galler, K. Bräutigam, C. Große, J. Popp, U. Neugebauer, Making a big thing of a small cell – recent advances in single cell analysis, Analyst 139 (2014) 1237–1273.

[8] L. Armbrecht, P.S. Dittrich, Recent advances in the analysis of single cells, Anal. Chem. 89 (2017) 2–21.

[9] L. Cid-Barrio, D. Bouzas-Ramos, A. Salinas-Castillo, Y. Ogra, J. Ruiz Encinar, J.M. Costa-Fernandez, Quantitative assessment of cellular uptake and differential toxic effects of HgSe nanoparticles in human cells, J. Anal. At. Spectrom. 35 (2020) 1979–1988.

[10] S. Theiner, K. Loehr, G. Koellensperger, L. Mueller, N. Jakubowski, Single-cell analysis by use of ICP-MS, J. Anal. At. Spectrom. 35 (2020) 1784–1813.

[11] A. Loukanov, P. Mladenova, S. Toshev, A. Karailiev, E. Ustinovich, S. Nakabayashi, Real time monitoring and quantification of uptake carbonnanodots in eukaryotic cells, Microsc. Res. Tech. 81 (12) (2018) 1541–1547.

[12] V.L. Dressler, D. Pozebon, M.F. Mesko, A. Matusch, U. Kumtabtim, B. Wu, J. Sabine Becker, Biomonitoring of essential and toxic metals in single hair using on-line solution-based calibration in laser ablation inductively coupled plasma mass spectrometry, Talanta 82 (5) (2010) 1770–1777.

[13] R. Weiskirchen, S. Weiskirchen, P. Kim, R. Winkler, Software solutions for evaluation and visualization of laser ablation inductively coupled plasma mass spectrometry imaging (LA-ICP-MSI) data: a short overview, J. Cheminf. 11 (1) (2019).

[14] M. Cruz-Alonso, A. Lores-Padín, E. Valencia, H. González-Iglesias, B. Fernández, R. Pereiro, Quantitative mapping of specific proteins in biological tissues by laser ablation-ICP-MS using exogenous labels: aspects to be considered, Anal. Bioanal. Chem. 411 (3) (2019) 549–558.

[15] A. Limbeck, P. Galler, M. Bonta, G. Bauer, W. Nischkauer, F. Vanhaecke, Recent advances in quantitative LA-ICP-MS analysis: challenges and solutions in the life sciences and environmental chemistry, Anal. Bioanal. Chem. 407 (2015) 6593–6617.

[16] T. Van Acker, T. Buckle, S.J.M. Van Malderen, D.M. van Willigen, V. van Unen, F.W.B. van Leeuwen, F. Vanhaecke, High-resolution imaging and single-cell analysis via laser ablation-inductively coupled plasma-mass spectrometry for the determination of membranous receptor expression levels in breast cancer cell lines using receptor-specific hybrid tracers, Anal. Chim. Acta 1074 (2019) 43–53.

[17] C. Giesen, H.A.O. Wang, D. Schapiro, N. Zivanovic, A. Jacobs, B. Hattendorf, P.J. Schüffler, D. Grolimund, J.M. Buhmann, S. Brandt, Z. Varga, P.J. Wild, D. Günther, B. Bodenmiller, Highly multiplexed imaging of tumor tissues with subcellular resolution by mass cytometry, Nat. Methods 11 (2014) 417–422.

[18] B. Bodenmiller, Multiplexed epitope-based tissue imaging for discovery and healthcare applications, Cell Syst. 2 (2016) 225–238.

[19] A. Arakawa, N. Jakubowski, G. Koellensperger, S. Theiner, A. Schweikert, S. Flemig, D. Iwahata, H. Traub, T. Hirata, Quantitative imaging of silver nanoparticles and essential elements in thin sections of fibroblast multicellular spheroids by high resolution laser ablation inductively coupled plasma time-of- flight mass spectrometry, Anal. Chem. 91 (2019) 10197–10203.

[20] J. Pisonero, D. Bouzas-Ramos, H. Traub, B. Cappella, C. Alvarez-Llamas, S. Richter, J.C. Mayo, J.M. Costa-Fernandez, N. Bordel, N. Jakubowski, Critical evaluation of fast and highly resolved elemental distribution in single cells using LA-ICP-SFMS, J. Anal. At. Spectrom. 34 (2019) 655-633.

[21] H.J. Stärk, R. Wennrich, A new approach for calibration of laser ablation inductively coupled plasma mass spectrometry using thin layers of spiked agarose gels as references, Anal. Bioanal. Chem. 399 (6) (2011) 2211–2217.

[22] M. Šala, V.S. Šelih, J.T. van Elteren, Gelatin gels as multi-element calibration standards in LA-ICP-MS bioimaging: fabrication of homogeneous standards and microhomogeneity testing, Analyst 142 (2017) 3356–3359.

[23] D. Drescher, C. Giesen, H. Traub, U. Panne, J. Kneipp, N. Jakubowski, Quantitative imaging of gold and silver nanoparticles in single eukaryotic cells by LA-ICP-MS, Anal. Chem. 84 (2012) 9684–9688.

[24] K. Lohr, O. Borovinskaya, G. Tourniaire, l. Panne, N. Jakubowski, Arraying of single cells for quantitative high throughput LaserAblation ICP-TOF-MS, Anal. Chem. 91 (2019) 11520–11528.

[25] A. Arakawa, N. Jakubowski, S. Flemig, G. Koellensperger, M. Rusz, D. Iwahata, H. Traub, T. Hirata, High-resolution laser ablation inductively coupled plasma mass spectrometry used to study transport of metallic nanoparticles through collagen-rich microstructures in fibroblast multicellular spheroids, Anal. Bioanal. Chem. 411 (2019) 3497–3506.

[26] I. Kroslakova, D. Günther, Elemental fractionation in laser ablation-inductively coupled plasma-mass spectrometry: evidence for mass load induced matrix effects in the ICP during ablation of a silicate glass, J. Anal. Atomic Spectrom. 22 (1) (2007) 51–62.

[27] Y.K. Hsieh, H.A. Hsieh, H.F. Hsieh, T.H. Wang, C.C. Ho, P.P. Lin, C.F. Wang, Using laser ablation inductively coupled plasma mass spectrometry to characterize the biointeractions of inhaled CdSe quantum dots in the mouse lungs, J. Anal. At. Spectrom. 28 (2013) 1396–1401.

[28] T.H. Wang, H.A. Hsieh, Y.K. Hsieh, C.S. Chiang, Y.C. Sun, C.F. Wang, The in vivo biodistribution and fate of CdSe quantum dots in the murine model: a laser ablation inductively coupled plasma mass spectrometry study, Anal. Bioanal. Chem. 404 (2012) 3025–3036.

[29] Qdot® ITK™ Carboxyl Quantum Dots Thermo Fisher scientific https://assets.thermofisher.com/TFS-Assets/LSG/manuals/mp19020.pdf sOctober 2020

[30] A.M. Smith, H. Duan, A.M. Mohs, S. Nie, Bioconjugated quantum dots for in vivo molecular and cellular imaging, Adv. Drug Deliv. Rev. 60 (2008) 1226–1240.

[31] M. Wang, L.N. Zheng, B. Wang, H.Q. Chen, Y.L. Zhao, Z.F. Chai, H.J. Reid, B.L. Sharp, W.Y. Feng, Quantitative analysis of gold nanoparticles in single cells by laser ablation inductively coupled plasma-mass spectrometry, Anal. Chem. 86 (2014) 10252–10256.

[32] X. Yun, M. Tang, Z. Yang, J.J. Wilksch, P. Xiu, H. Gao, F. Zhang, H. Wang, Interrogation of drug effects on HeLa cells byexploiting new AFM mechanical biomarkers, RSC Adv. 7 (2017) 43764.

[33] X. Jiang, C. Röcker, M. Hafner, S. Brandholt, R.M. Dörlich, G. Ulrich Nienhaus, Endo- and exocytosis of zwitterionic quantum dot nanoparticles by live HeLa cells, ACS Nano 4 (2010) 6787–6797.

[34] L.N. Zheng, M. Wang, B. Wang, H.Q. Chen, H. Ouyang, Y.L. Zhao, Z.F. Chai, W.Y. Feng, Determination of quantum dots in single cells by inductively coupled plasma mass spectrometry, Talanta 116 (2013) 782–787.

[35] S. Ashraf, J. Park, M.A. Bichelberger, K. Kantner, R. Hartmann, A.H. Said, N. Feliu, J. Lee, D. Lee, G.U. Nienhaus, S. Kim, W.J. Parak, Zwitterionic surface coating of quantum dots reduces protein adsorption and cellular uptake, Nanoscale 8 (2016) 17794–17800.